SEMARAK ILMU PUBLISHING

Semarak International Journal of Nanotechnology

Journal homepage:
https://semarakilmu.my/index.php/sijn/index
ISSN: 3030-6604

Molecular Insight into Functionalised Fumed Silica–PVDF Interactions: A Simulation-Based Approach for Understanding Filler–Polymer Compatibility in MMMs

Aishah Rosli[1,2,*], Nur Dina Zaulkiflee[3,4], Low Siew Chun[4], Abdul Latif Ahmad[4], Muhammad Abbas Ahmad Zaini[1,2], Mazura Jusoh[1,2]

[1] Faculty of Chemical and Energy Engineering, Universiti Teknologi Malaysia, 81310, UTM Johor Bahru, Johor, Malaysia
[2] Centre of Lipids Engineering & Applied Research (CLEAR), Ibnu-Sina Institute for Scientific & Industrial Research (ISI-SIR), Universiti Teknologi Malaysia, 81310 UTM Johor Bahru, Johor, Malaysia
[3] Graduate School of Engineering Science, Osaka University, Toyonaka, Osaka 560-8531, Japan
[4] School of Chemical Engineering, Engineering Campus, Universiti Sains Malaysia, Seri Ampangan, 14300, Nibong Tebal, Pulau Pinang, Malaysia

ARTICLE INFO

Article history:
Received 30 April 2025
Received in revised form 15 May 2025
Accepted 25 June 2025
Available online 30 June 2025

Keywords:
Molecular simulation; polymer–filler compatibility; functionalised silica nanoparticles; mixed matrix membranes

ABSTRACT

Silica nanoparticles, one of the fillers that have been used in mixed matrix membranes, can be functionalised to increase its compatibility with polymer matrices of the membrane. However, the molecular interactions that govern this compatibility are often poorly understood and difficult to assess prior to fabrication. This work aims to assess the interaction strength between silica fillers that have been functionalised with three organosilicon dubbed TS-530, TS-610, and TS-720 and polyvinylidene fluoride (PVDF) membrane matrix using molecular simulation. It is desired to determine whether computation modelling can reliably predict filler-polymer compatibility by comparing with experimental observations. Therefore, geometry optimisations and binding energy calculations were done using MM+, AM1, and PM3 methods in HyperChem 8.0 software. Each silica surface was modelled as a functionalised silanol core that has been treated with HMDS, DMDCS, and PDMS, representing TS-530, TS-610, and TS-720 functionalised silica nanoparticles respectively, then paired with a PVDF oligomer as the membrane matrix. The simulation results showed that TS-530 exhibited the most favourable interaction with PVDF, with the strongest binding energy and the most consistent surface contact. On the other hand, TS-610 and TS-720 showed weaker and more localised interactions with PVDF. These results are consistent with the experimental results for the mixed matrix PVDF membranes with functionalised silica nanoparticles as fillers. TS-530 mixed matrix membranes showed more uniform nanoparticle dispersion, higher contact angle and LEP_w values, signifying better membrane wetting resistance. Additionally, it showed superior CO_2 permeability and selectivity compared to other mixed matrix membranes. This study demonstrates that it is possible to use molecular modelling to effectively predict polymer-filler compatibility in membrane materials. The ability to predict dispersion and interface behaviour from simulated interaction energies offers a valuable screening tool for selection of materials for membrane design.

* *Corresponding author.*
E-mail address: aishahrosli@utm.my

https://doi.org/10.37934/sijn.5.1.113

1. Introduction

Mixed matrix membranes (MMMs) have become attractive candidates for carbon dioxide (CO_2) separation attributing to their ability to combine the advantageous properties of both polymers and inorganic fillers. Among the common polymers used for membrane fabrication, polyvinylidene fluoride (PVDF) offers good chemical resistance, high mechanical and thermal stability, and is easy to process [1]. The addition of silica nanoparticles into PVDF-based membranes to improve performance in terms of permeability, selectivity, structure, and wetting resistance has been investigated by several researchers prior [2-4]. In a previous research, fumed silica nanoparticles that have been functionalised with organosilanes, such as hexamethyldisilazane (HMDS), dimethyldichlorosilane (DMDCS), and polydimethylsiloxane (PDMS) have been incorporated into membranes to tailor the surface energy and hydrophobicity of silica nanoparticles. These commercially available variants of silica nanoparticles typically differ in their surface chemistries and have shown differing effects on membrane performance in experimental studies. Even though some functionalisation of silica nanoparticles showed good promise, leading to improved dispersion in the membrane matrix, anti-wetting behaviour, and augmented gas absorption flux, some functionalised silica nanoparticles suffered from aggravated agglomeration and reduced selectivity [5]. The stark differences in performance of the functionalised silica-based MMMs are presumed to be due to variations in the interactions between the polymer and the silica fillers, but a molecular-level understanding of these interactions remains lacking.

To date, the interface between functionalised silica nanoparticles and polymer matrix has been largely inferred by analysis and tests such as macroscopic characterisation methods such as scanning electron microscopy (SEM), contact angle measurements, atomic force microscopy (AFM), and gas permeation tests, to name a few [5]. While these methods can provide indirect evidence of the compatibility and dispersion of the nanoparticles within the MMMs, they cannot directly probe the nature of non-covalent interactions or binding affinities at the molecular level. As such, there is a lack of understanding on how the surface chemistry affects the microscopic interaction between functionalised silica nanoparticles and polymer chains.

Therefore, this study aims to bridge that gap by conducting a comparative molecular simulation study on the interaction between PVDF oligomers and various functionalised silica nanoparticles. Using molecular mechanics and semi-empirical methods, the binding energies, interaction geometries, and surface affinities are quantified and illustrated to reveal how silica nanoparticles with different functional groups on the surface affect their compatibility with PVDF membrane matrix. The simulation results are further supported and interpreted using experimental data, providing mechanistic rationale for the observed impact on membrane morphology, wettability, and CO_2 separation performance. This study provides a molecular-level perspective that can guide the rational selection and design of fillers for advanced MMM applications.

2. Methodology

2.1 Computational Method

In this study, three types of functionalised fumed silica nanoparticles were represented by molecular fragments mimicking the surface chemistry of TS-530, TS-610, and TS-720. These are commercial silica products treated with HMDS, DMDCS, and PDMS, respectively. For each type, a silica-based core fragment was constructed and capped with the corresponding surface-modifying groups to reflect the dominant functional chemistry.

The polymer matrix was represented by an oligomer of PVDF, consisting of five repeating –(CH_2–CF_2)– units. This chain length is sufficient to capture local conformational behaviour and interaction trends, while remaining computationally manageable for the optimisation process.

All molecular structures were built and pre-optimised using HyperChem 8.0 and arranged such that the PVDF oligomer was placed in close proximity to the surface-modified silica fragment. Care was taken to vary the initial orientation of the PVDF chain to allow for exploration of multiple local minima during optimisation.

Molecular mechanics (MM+) was first used to perform geometry optimisation of the combined polymer–filler system. This method accounts for van der Waals and electrostatic interactions and is suitable for estimating interaction energies and equilibrium conformations in large, non-reactive molecular systems. To refine the interaction energy estimates, semi-empirical methods (AM1 and PM3) were also employed on select configurations.

Each system was optimised under vacuum conditions using the Polak–Ribiere conjugate gradient algorithm with an RMS gradient convergence limit of 0.01 kcal/(mol·Å). Binding energy (ΔE) between the PVDF oligomer and the silica fragment was calculated using the Eq. (1) as follows:

$$\Delta E = E_{total} - (E_{PVDF} + E_{silica}) \quad (1)$$

Where E_{total} is the minimised energy of the combined system, and E_{PVDF} and E_{silica} are the minimised energies of the isolated PVDF oligomer and silica fragment, respectively. A more negative ΔE indicates a stronger interaction.

Each simulation was repeated using at least three different initial orientations of the PVDF chain to ensure the robustness of the interaction trends and to avoid artifacts from local energy minima.

2.2 Experimental Method

2.2.1 Materials

Polyvinylidene fluoride (PVDF, Solvay Solexis, France) was used as the polymer to fabricate the membrane, dissolved into N-methyl-2-pyrrolidone (NMP, Sigma–Aldrich, Germany) and immersed in ethanol (Merck, Germany) coagulation bath. Three SiNP that have been functionalised with different organosilicon; hexamethyldisilane (HMDS), dimethyldichlorosilane (DMDCS), and polydimethylsiloxane (PDMS) were provided courtesy of Cabot Inc., dubbed as TS-530 f-SiNP (HMDS), TS-610 f-SiNP (DMDCS), and TS-720 f-SiNP (PDMS) respectively. For the gas separation tests, AMP from Merck, was used as the liquid absorbent.

2.2.2 Membrane synthesis

A total of 15 wt% dried PVDF was gradually dissolved in pre-heated NMP solvent maintained at 60 °C, with continuous stirring at 250 rpm for 6 hours. The resulting dope solution was allowed to cool to room temperature before undergoing sonication to eliminate entrapped air bubbles. It was then cast onto a glass plate using a thin film applicator with a casting gap of 400 µm. The cast film was immediately immersed in a coagulation bath consisting of 20/80 v/v ethanol/water for 24 hours, followed by drying for 3 days to produce the neat membrane [5].

Nanocomposite membranes were prepared using a solution blending method. A 1 wt% loading of LDPE/f-SiNP, relative to 15 wt% PVDF, was first dispersed in NMP and stirred for 30 minutes. This mixture was then sonicated for another 30 minutes to enhance nanoparticle dispersion. Approximately 10% of the total PVDF was added and sonicated for an additional 30 minutes before

gradually incorporating the remaining polymer [6]. The resulting solution was cast and solidified following the same procedure used for the neat membrane.

2.2.3 Membrane characterisation

The morphology of the fabricated membranes was examined using a TM3000 Table Top scanning electron microscope (SEM, Hitachi, Japan). Prior to imaging, membrane samples were fractured in liquid nitrogen and sputter-coated with gold to enhance surface conductivity. Elemental analysis of silicon within the membrane was conducted using energy-dispersive X-ray spectroscopy (EDS). EDS line scanning and mapping were employed to assess the dispersion of functionalised silica nanoparticles (f-SiNP) throughout the membrane structure.

ImageJ software was used to evaluate the pore size distribution based on SEM surface images. The scale bar in each micrograph was used to calibrate measurement settings, and a thresholding technique was applied to binarise the image, allowing clear differentiation between membrane pores and the polymer matrix. The surface wettability of the membranes was determined using a contact angle goniometer (Rame-Hart 250 F-1, USA) via the sessile drop method. Water droplets were dispensed at multiple locations on the membrane surface using a micro-syringe, and the average contact angle was calculated to minimise measurement variability.

Liquid entry pressure of water (LEP_w) was measured using a Porolux 1000 porometer (Benelux Scientific, Belgium) based on the bubble point method. Membrane samples were cut into 2.5 cm diameter discs and placed into the sample holder. A water layer was applied to the membrane surface before sealing, and nitrogen gas was introduced in incremental pressure steps of 0.1 bar. The LEP_w value was recorded as the pressure at which the first liquid flow was observed [7]. Fourier-transform infrared (FTIR) spectroscopy (Nicolet iS10, Thermo Scientific) was used to identify chemical features associated with the different f-SiNP types and to detect changes in membrane chemical composition resulting from nanoparticle incorporation.

2.2.3 MGA performance test

The experiment was performed at atmospheric pressure and room temperature using the MGA settings shown in our previous work [4]. In the MGA system, 100 mL/min of pure CO_2 feed gas was used, and 100 mL/min of MEA was used as the liquid absorbent. Before evaluating the separation performance, let the system run for 15 minutes to achieve a steady state. The CO_2 absorption flux, J_{CO2} (mol/m^2.s), was calculated using Eq. (2), where the flow rates of the inlet and retentate gas were measured by a bubble soap meter.

$$J_{CO_2} = \frac{(Q_{g,i} - Q_{g,r})\rho_g}{MW_g A} \quad (2)$$

Where $Q_{g,i}$ is the inlet gas flow rate (mL/min), $Q_{g,r}$ is the retentate gas flow rate (mL/min), ρ_g is the density of CO_2 (g/mL), MW_g is the molecular weight of CO_2 (g/mol), and A is the membrane contacting area (m^2). CO_2:N_2 with a volume ratio of 20:80 was also used for a 120 hour binary gas absorption operation to give a more realistic view of a long-term MGA operation. The CO_2 flux was calculated based on the retentate gas composition analysed by the gas chromatography system.

3. Results and Discussions

3.1 Optimised Molecular Structures

The optimised geometries of PVDF interacting with three functionalised silica fragments—TS-530, TS-610, and TS-720—are shown in Figure 1. These fragments were modeled by functionalising silanol-terminated silica cores with hexamethyldisilazane (HMDS), dimethyldichlorosilane (DMDCS), and polydimethylsiloxane (PDMS), respectively. Optimisations were performed using MM+, AM1, and PM3 semi-empirical methods within the HyperChem 8.0 suite. For each silica/PVDF system, three distinct initial orientations of the PVDF oligomer were evaluated, and the configuration exhibiting the lowest total energy was selected for detailed structural analysis. The resulting non-bonded contact distances and qualitative polymer conformations are summarised in Table 1, while the final optimised geometries are illustrated in Figure 1 (a–c).

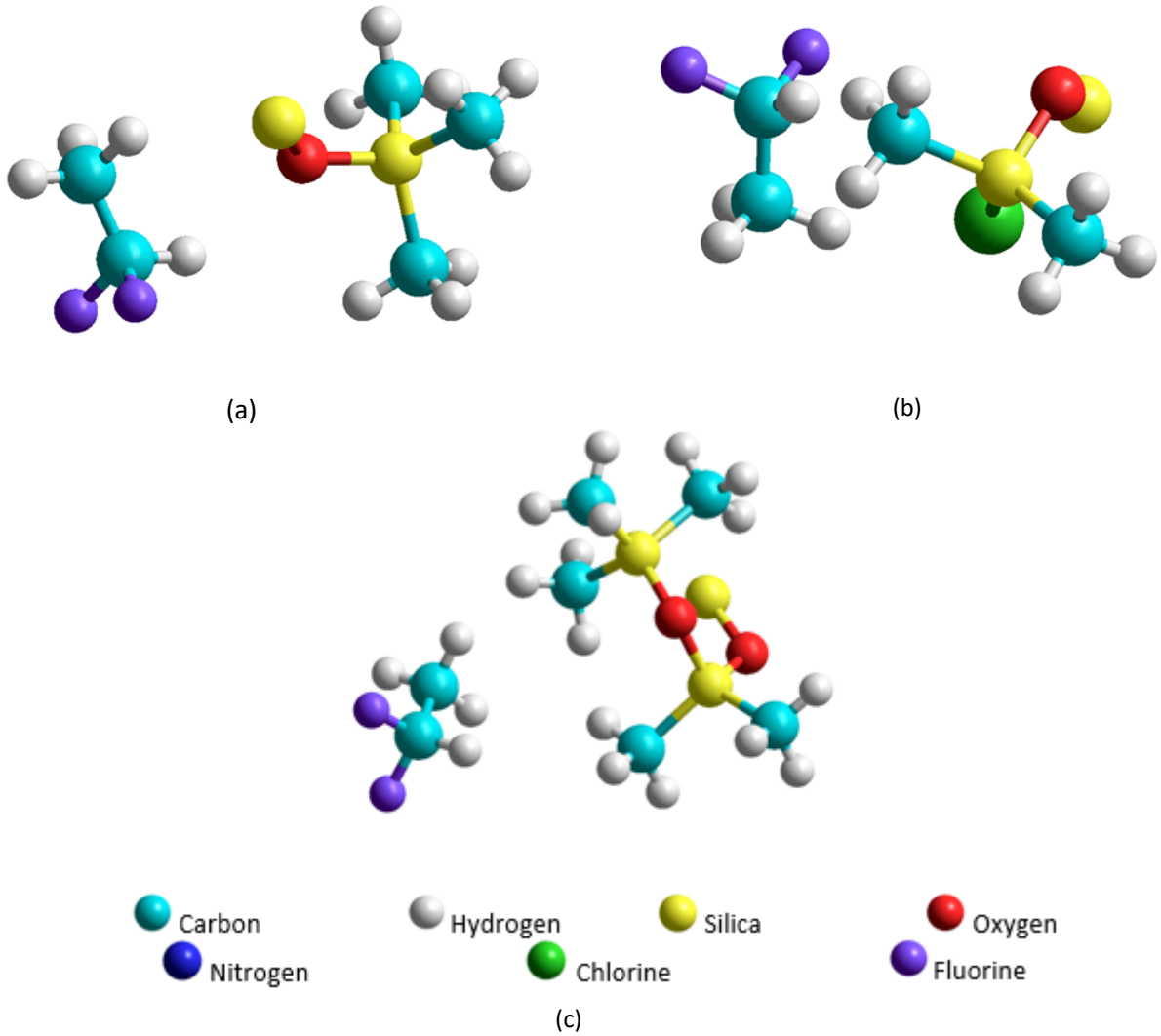

Fig. 1. Optimised structures of PVDF interacting with (a) TS-530, (b) TS-610, and (c) TS-720 functionalised silica fragments

Table 1
Summary of PVDF–silica structural observations from the optimised configurations with the lowest binding energy (ΔE)

Filler type	Surface functional group	PVDF orientation	Contact area	Closest distance (Å)
TS-530	$–Si(CH_3)_3$	Parallel	Broad	2.56
TS-610	$–Si(CH_3)_2Cl$	Slightly angled	Limited	1.72
TS-720	$–Si(CH_3)_2–O–$	Angled	Partial	2.67

In the TS-530 system (Figure 1a) the PVDF oligomer aligned parallel to the HMDS-modified silica surface, with a minimum non-bonded contact distance of 2.56 Å. This geometry suggests favourable van der Waals interactions between the hydrophobic $–CF_2$ groups of PVDF and the $–Si(CH_3)_3$ termini of the surface. A similar parallel alignment was observed in earlier simulations of LDPE-coated silica, where methylated groups contributed to uniform surface coverage and reduced nanoparticle agglomeration [4]. Although PVDF is more polar and rigid than LDPE, the comparable alignment in this case reinforces the affinity between methylated surfaces and hydrocarbon/fluorocarbon polymers. Furthermore, recent work on nanosilica/LDPE composites documents that methylated surfaces improve filler dispersion and interfacial interaction, significantly enhancing mechanical strength and thermal stability [8]. In contrast, the PVDF oligomer interacting with the DMDCS-functionalised TS-610 (Figure 1b) adopted a slightly angled conformation, maintaining a closest contact distance of 1.72 Å. Despite the short contact point, the overall contact area was limited, suggesting a localized interaction. This may be due to steric or polar repulsion from the chlorosilane-modified surface, which could reduce polymer wrapping or anchoring. These findings align with prior reports of TS-610 agglomeration in PVDF-based membranes, where poor surface compatibility compromised dispersion and membrane morphology [4].

In the TS-720 system (Figure 1c), the PVDF chain was observed to lie at an angle to the PDMS-functionalised silica surface, with a minimum contact distance of 2.67 Å. The flexible $–Si(CH_3)_2–O–$ siloxane chains introduce steric bulk and surface fluidity, which limit stable, close-packed alignment with the rigid PVDF backbone. Recent studies on PVDF/PDMS hybrid membranes report that PDMS flexibility can disrupt uniform polymer–filler contact, leading to inconsistent interfacial adhesion [9]. Moreover, studies on PDMS/PVDF composite systems designed for pervaporation and butanol recovery reveal that although PDMS may enhance hydrophobicity and selective permeability, its mechanical flexibility can undermine interfacial cohesion and structural integrity at the polymer–matrix boundary. For instance, Pan *et al.,* [10] demonstrated that while PDMS films supported on PVDF substrates yield defect-free coatings, excessive PDMS flexibility reduces interfacial toughness and disrupts coherent adhesion. Despite the hydrophobic nature of PDMS, its chain-like structure may have created inconsistent contact regions and restricted effective interaction. Similar steric interference was discussed by Rosli *et al.,* [4], where PDMS flexibility prevented coherent contact in LDPE coating models. These conformational differences provide insight into how surface functionalisation affects filler–polymer geometry. The relatively parallel and broad alignment in the TS-530 system suggests greater compatibility with PVDF, while angled or distorted configurations observed in TS-610 and TS-720 may correspond to weaker interfacial interaction. An interpretation explored further in Section 3.2.

3.2 Binding Energy Analysis

The interaction energies (ΔE) between PVDF oligomer and each functionalised silica fragment (TS-530, TS-610, and TS-720) were calculated using MM+, AM1, and PM3 methods, as previously described. A more negative ΔE value indicates a stronger and more energetically favourable

interaction between the polymer and the filler. The binding energies for the most stable configurations of each system are summarised in Table 2.

Table 2
Calculated binding energies (ΔE) between PVDF and each functionalised silica surface using three different methods

System	Method	ΔE (kcal/mol)
TS-530 in PVDF membrane	MM+	-2.6884
	AM1	-11.8457
	PM3	-26.6619
TS-610 in PVDF membrane	MM+	-0.6172
	AM1	-3.6232
	PM3	-30.2135
TS-720 in PVDF membrane	MM+	-0.1582
	AM1	-23.5716
	PM3	-42.2843

Across all three methods, the TS-530 system exhibited the most favourable interaction with PVDF, with the lowest ΔE values recorded in each case (Table 2). This result is consistent with the broad, parallel alignment observed in the optimised structure (Figure 1a), which maximises surface contact between the $–CF_2$ groups of PVDF and the methylated $–Si(CH_3)_3$ surface of the silica. The consistency across both MM+ and AM1 methods reinforces the interpretation that TS-530 presents the most compatible surface chemistry among the three fillers. This conclusion aligns with recent atomistic simulations showing that HMDS-functionalisation of silica significantly improves nanoparticle dispersion and enhances interfacial adhesion in polyethylene-based systems. For instance, Genix et *al.,* [11] reported that alkyl-silane grafting on silica nanoparticles yielded more stable polymer interlayers and reduced aggregation in nanocomposites, while Saito *et al.,* [12] found enhanced interfacial affinity and adhesion between functionalised alumina and polymer matrices following similar grafting strategies. These findings collectively underscore the robust efficacy of HMDS grafting in promoting strong interfacial interactions in polymer–silica composites.

In contrast, the TS-610 system, exhibited weaker interactions across all methods. Its functional group $–Si(CH_3)_2Cl$ introduces greater polarity and potential steric hindrance compared to TS-530, which may explain the less favourable binding energies. The PVDF chain was observed to interact at a slight angle and with limited surface contact (Figure 1b), which aligns with the reduced ΔE values. In the case of TS-720, the results were more method-dependent. MM+ predicted the weakest interaction (–0.158 kcal/mol), consistent with the angled and partially detached configuration shown in Figure 1c. However, AM1 and PM3 gave unexpectedly high binding strengths (–23.572 and –45.284 kcal/mol, respectively). These values may reflect overestimated polar interactions or polarisability effects introduced by the flexible PDMS chains. Despite this numerical anomaly, the observed geometry and physical behaviour suggest that PVDF–TS-720 compatibility is lower than that of TS-530. Molecular simulations and experimental studies of PDMS–silica interfaces consistently show that although PDMS may improve hydrophobicity, its high chain mobility and polarisability often reduce effective adhesion and interfacial cohesion [13].

These trends mirror earlier observations in LDPE-coated silica simulations [4], where HMDS-functionalised surfaces facilitated stronger interfacial adhesion due to steric compatibility and hydrophobic interactions. The current findings also correlate with experimental membrane studies by Rosli *et al.,* [5] in which TS-530-enhanced PVDF membranes demonstrated better dispersion and higher resistance to wetting attributes likely linked to stronger molecular interactions at the polymer–filler interface. In contrast, the polar TS-610 surface and flexible TS-720 (PDMS) surface

both show weaker interaction potentials, which may lead to filler aggregation, poor dispersion, and compromised membrane performance. Pang *et al.,* [14] showed that PVDF–SiO_2–HDTMS membranes maintained high tensile strength and CO_2 absorption performance. This highlights that hydrophobic filler functionalisation can enhance performance only when strong interfacial cohesion is maintained, whereas flexible filler architectures like PDMS can undermine mechanical integrity if adhesion is discontinuous.

3.3 Nature of Interactions

To further interpret the observed differences in binding energy, the nature of the interactions between PVDF and each functionalised silica surface was examined qualitatively from the optimised molecular geometries. While the calculated ΔE values quantify overall interaction strength, visual inspection of the spatial arrangement and proximity between functional groups offers insight into the underlying mechanisms governing compatibility. In the TS-530 system, the PVDF chain interacts with a surface functionalised by $–Si(CH_3)_3$ groups from HMDS treatment. These methyl groups present a low-polarity, hydrophobic surface that complements the semi-fluorinated PVDF chain [15]. The optimised geometry shows multiple $–CF_2$ units aligned along the methylated silica surface, enabling consistent van der Waals contacts. This widespread interaction zone, seen in Figure 1(a), supports the relatively strong and evenly distributed binding energy observed across all three computational methods. Similar methyl-based surface interactions were previously noted in an earlier work involving LDPE–TS-530 simulations [4], which also highlighted the importance of chain flexibility and surface coverage.

For the TS-610 system, the silica surface was functionalised with $–Si(CH_3)_2Cl$ groups. The presence of the chlorine atom introduces localised polarity, and its larger van der Waals radius may limit close packing with the PVDF backbone. The PVDF chain, while able to approach the surface more closely at a single point (1.72 Å), shows a more restricted contact region, with fewer $–CF_2$ groups engaging simultaneously. This likely reflects a mixture of steric hindrance and weaker dispersion interaction, leading to less favourable ΔE values and partial surface alignment (Figure 1b). The TS-720 system presents a more complex case. Functionalisation with PDMS introduces flexible $–Si(CH_3)_2–O–$ repeat units that extend outward from the silica surface. Although PDMS is hydrophobic, the flexibility and spatial mobility of its chains may disrupt stable PVDF alignment [16]. As seen in Figure 1(c), the PVDF oligomer adopts an angled configuration with partial contact, and the interaction area appears fragmented. Despite the surprisingly strong ΔE values predicted by AM1 and PM3, this may be an artifact of enhanced polarisability or dynamic charge redistribution, which these semi-empirical methods are known to overemphasise in soft, non-rigid systems. From a structural perspective, the physical contact between PVDF and the PDMS layer appears less coherent than in the TS-530 system, suggesting weaker practical adhesion.

Although across all systems, evidence of hydrogen bonding was observed, it may not be the prevailing mechanism, as the PVDF backbone lacks proton donors and the surface groups either lack suitable acceptors or are sterically inaccessible. Instead, the primary interaction mechanisms appear to be van der Waals forces, steric compatibility, and, to a lesser extent, dipolar alignment [17]. These differences help explain the relative binding strengths and set the foundation for linking simulation outcomes to experimental membrane performance.

3.4 Correlation with Experimental Observations

The molecular interaction trends identified in this simulation study correspond closely with experimental outcomes for PVDF membranes incorporating TS-530, TS-610, and TS-720 silica fillers. In particular, differences in filler dispersion, surface wettability, and gas separation performance can be linked to the computed binding energies and interaction geometries discussed in Sections 3.2 and 3.3.In the case of TS-530, simulation results revealed a parallel and extensive contact between the PVDF chain and the methylated silica surface, resulting in the strongest binding energy among the three systems. This correlates well with the experimental results shown in Figure 2, where the FESEM cross-sectional image (Figure 2a) displays a dense, well-structured membrane morphology and the EDX silica mapping (Figure 2d) shows uniformly distributed nanoparticles across the membrane surface [18]. In contrast, TS-610 exhibited a more limited and angled interaction in simulation, which is reflected in Figure 2(b) as localised clusters and a more porous substructure. The corresponding EDX map (Figure 2e) confirms the presence of silica aggregates and uneven surface distribution. TS-720, which had the weakest interaction in simulation, shows a similarly disrupted membrane structure (Figure 2c) and the most uneven particle dispersion in the EDX map (Figure 2f), with clear evidence of particle clustering. These results reinforce the simulation-derived compatibility ranking of TS-530 > TS-610 > TS-720.

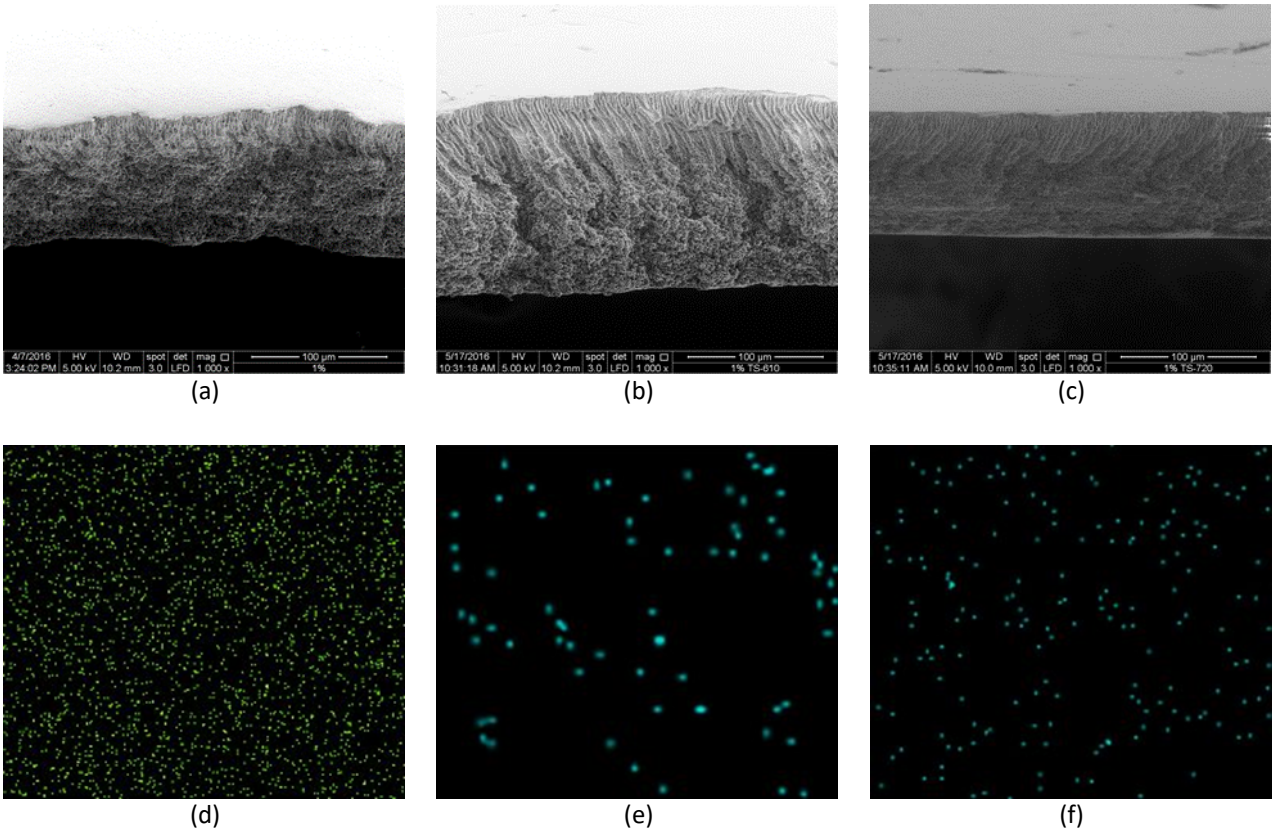

Fig. 2. Cross-sectional FESEM images (top row) and EDX silica surface mapping (bottom row) of PVDF mixed matrix membranes incorporating 1 wt% of different functionalised silica nanoparticles: (a, d) TS-530, (b, e) TS-610, and (c, f) TS-720.

The superior PVDF–TS-530 interaction observed in simulation is also reflected in membrane wettability characteristics. As shown in Table 3, the membrane incorporating TS-530 exhibited the highest contact angle (90.4° ± 0.5°) and the greatest LEP_w (7.51 bar), indicating enhanced surface

hydrophobicity and greater resistance to wetting. In contrast, membranes containing TS-610 and TS-720 demonstrated much lower contact angles (54.1° and 61.3°, respectively) and LEP_w values around 3 bar. These results support the view that stronger molecular-level interactions between PVDF and the HMDS-functionalised TS-530 promote better surface compatibility and coverage, leading to reduced membrane wettability [19]. The weaker adhesion and surface contact observed in TS-610 and TS-720 systems in simulation likely contribute to localised voids or defects that increase water intrusion under pressure [20].

Table 3
Contact angle and LEP_w data at 1 wt% silica loading

System	Contact angle (°)	LEP_w (bar)
TS-530 in PVDF membrane	90.4 ± 0.5	7.51
TS-610 in PVDF membrane	54.1 ± 1.0	3.00
TS-720 in PVDF membrane	61.3 ± 0.7	3.03

FTIR analysis further supports the simulation-derived differences in polymer–filler interaction. As shown in Figure 3, membranes containing TS-530 exhibited unique or shifted absorption bands compared to both pristine PVDF and the other filled membranes, particularly at 1029 and 1122 cm^{-1}, corresponding to Si–O–Si vibrations from the HMDS-treated surface, and a broad low-energy band at 1068 cm^{-1}. A band at 1499 cm^{-1} was attributed to Si–N–H vibrations, while a broad Si–OH stretching band appeared at 3458 cm^{-1}, consistent with HMDS chemistry [21]. These shifts suggest subtle but significant chemical interaction or proximity effects between the silica surface and PVDF chains, consistent with the close alignment and strong binding observed in simulation. In contrast, membranes with TS-610 and TS-720 showed general absorption bands related to surface groups from DMDCS and PDMS treatment, including Si–OH stretching (3432 cm^{-1}), Si–CH_3 bending (1261 and 1442 cm^{-1}), and Si–O–Si or Si–OH deformation modes (e.g., 811, 952, and 1029 cm^{-1}), as reported in prior studies [22]. While these confirm successful incorporation of the treated silica nanoparticles into the PVDF matrix, the lack of distinctive new or shifted peaks compared to TS-530 indicates weaker interfacial interaction. These spectral differences reinforce the interpretation that only TS-530 forms a more integrated interfacial environment—matching the binding energy and geometry results predicted by HyperChem.

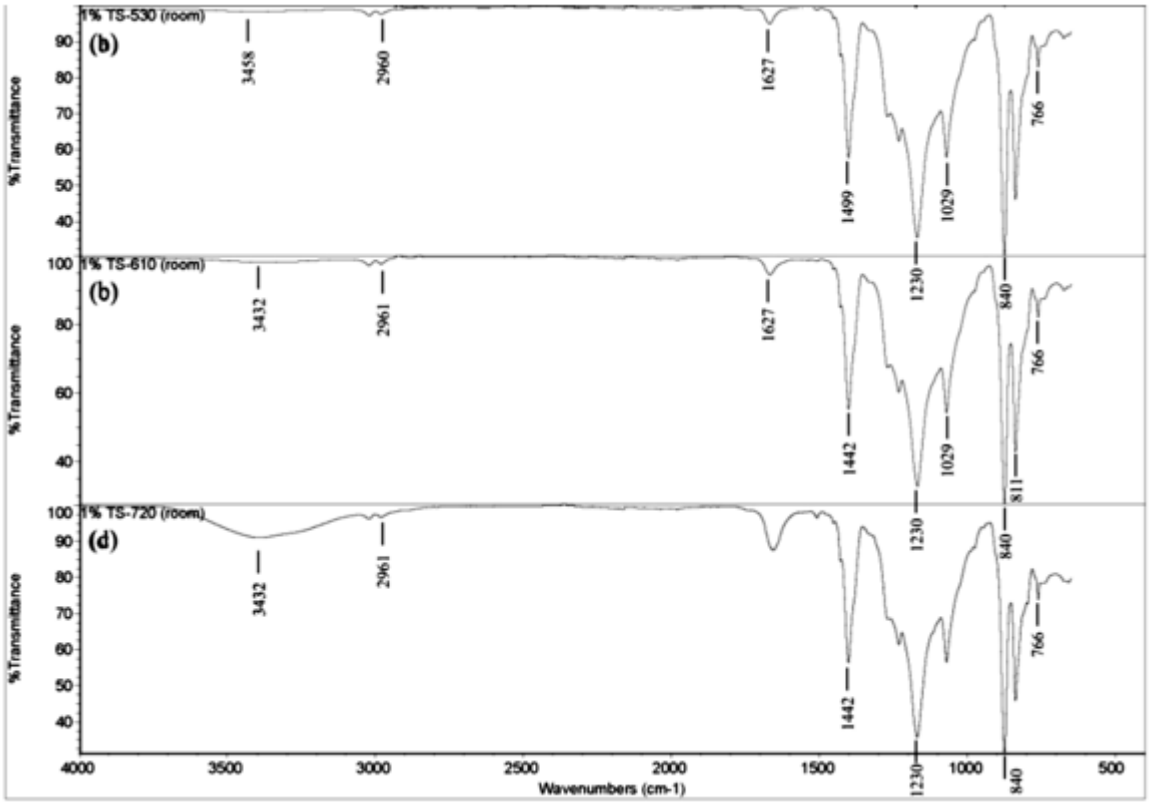

Fig. 3. FTIR spectra for (a) TS-530, (b) TS-610, and (d) TS-720 in PVDF composite membranes

Gas separation measurements further support the simulation-predicted differences in polymer–filler interaction strength. As shown by the experimental data, the PVDF membrane incorporating TS-530 exhibited the highest CO_2 permeability, approximately 1.91×10^{-4} mol/m²·s, and the highest CO_2/N_2 selectivity of around 22. This is consistent with results from Mamah *et al.,* [23] who demonstrated that PVDF–SiO_2–HDTMS hollow-fiber membranes engineered via NIPS retained over 97 % CO_2 flux and maintained robust mechanical properties, attributed to improved polymer–filler compatibility and minimal void formation. These values are notably higher than those of membranes containing TS-610 (1.65×10^{-4} mol/m²·s, selectivity ≈ 17) and TS-720 (1.40×10^{-4} mol/m²·s, selectivity ≈ 8). The superior performance of the TS-530 membrane aligns with its stronger simulated interaction energy (ΔE ≈ –11.85 kcal/mol via AM1) and broader surface contact in the optimised geometry. These factors likely enhance the filler–polymer interface integrity, suppress non-selective void formation, and maintain membrane structure under gas exposure. The moderate performance of the TS-610 membrane corresponds to its intermediate binding energy and limited contact area, while the low permeability and selectivity of the TS-720 membrane reflect its weaker interaction with PVDF and the disrupted surface contact seen in simulation. Similar trends were reported in Liu *et al.,* [24], where PDMS@ZIF-8/PVDF pervaporation membranes showed high flux but compromised mechanical stability due to incomplete polymer–filler interfaces. Together, the gas transport data reinforce the molecular modelling results and confirm that stronger polymer–filler interactions can translate into improved separation performance at the macroscale.

4. Conclusions

This study investigated the molecular interaction between PVDF and three functionalised silica nanoparticles—TS-530, TS-610, and TS-720—using MM+, AM1, and PM3 methods in HyperChem.

The objective was to evaluate how surface chemistry influences polymer–filler compatibility at the molecular level, and to determine whether simulation results could predict observed membrane performance. The results showed that the TS-530 system, functionalised with HMDS, exhibited the strongest interaction with PVDF, supported by both binding energy calculations ($\Delta E \approx -11.85$ kcal/mol via AM1) and favourable alignment in the optimised geometries. TS-610 and TS-720 demonstrated weaker interactions, with reduced surface contact and higher simulated distances. These differences in molecular compatibility were consistent with experimental observations: TS-530 membranes displayed more uniform silica dispersion, higher contact angle and LEP_w, and superior CO_2 permeability and selectivity compared to the other systems. The alignment between simulation and experiment demonstrates that molecular modelling can serve as an effective predictive tool for evaluating filler compatibility in membrane design. Specifically, interaction energy and surface geometry analysis can help pre-screen candidate materials for anti-wetting or separation applications. Future work may extend this approach to other polymers or functionalisation types or explore solvent effects and temperature influences in a broader simulation framework.

Acknowledgement
This research was funded by a grant from Ministry of Higher Education of Malaysia (FRGS Grant R.J130000.7824.4X172).

References

[1] Dallaev, Rashid, Tatiana Pisarenko, Dinara Sobola, Farid Orudzhev, Shikhgasan Ramazanov, and Tomáš Trčka. "Brief review of PVDF properties and applications potential." *Polymers* 14, no. 22 (2022): 4793. https://doi.org/10.3390/polym14224793

[2] Feng, Hui, Huijuan Li, Meng Li, and Xuan Zhang. "Construction of omniphobic PVDF membranes for membrane distillation: Investigating the role of dimension, morphology, and coating technology of silica nanoparticles." *Desalination* 525 (2022): 115498. https://doi.org/10.1016/j.desal.2021.115498

[3] Baghbanzadeh, Mohammadali, Dipak Rana, Christopher Q. Lan, and Takeshi Matsuura. "Effects of hydrophilic silica nanoparticles and backing material in improving the structure and performance of VMD PVDF membranes." *Separation and Purification Technology* 157 (2016): 60-71. https://doi.org/10.1016/j.seppur.2015.11.029

[4] Rosli, Aishah, Samuel Anand Stephen Paul, and Siew Chun Low. "Computational analysis of atomic binding energy for organosilicon-low-density polyethylene-coated silica embedded in polyvinylidene fluoride composite membrane for membrane gas absorption." *International Journal of Energy Research* 45, no. 10 (2021): 15372-15388. https://doi.org/10.1002/er.6810

[5] Rosli, Aishah, Abdul Latif Ahmad, and Siew Chun Low. "Enhancing membrane hydrophobicity using silica end-capped with organosilicon for CO2 absorption in membrane contactor." *Separation and Purification Technology* 251 (2020): 117429. https://doi.org/10.1016/j.seppur.2020.117429

[6] Ahmad, Abdul Latif, Aishah Rosli, Siew Chun Low, and Jit Kang Lim. "Effects of Silica loading on the absorption of carbon dioxide by mixed matrix membranes." *J Phys Sci* 29 (2018): 91-97. https://doi.org/10.21315/jps2018.29.s1.12

[7] Rácz, Gábor, Steffen Kerker, Zoltán Kovács, Gyula Vatai, Mehrdad Ebrahimi, and Peter Czermak. "Theoretical and experimental approaches of liquid entry pressure determination in membrane distillation processes." *Periodica Polytechnica: Chemical Engineering* 58, no. 2 (2014): 81-91. https://doi.org/10.3311/PPch.2179

[8] Alghdeir, Malek, Khaled Mayya, and Mohamed Dib. "Characterization of Nanosilica/Low-Density Polyethylene Nanocomposite Materials." *Journal of Nanomaterials* 2019, no. 1 (2019): 4184351. https://doi.org/10.1155/2019/4184351

[9] Huang, Jin, Jiajia Zhou, and Mingjie Liu. "Interphase in polymer nanocomposites." *JACS Au* 2, no. 2 (2022): 280-291. https://doi.org/10.1021/jacsau.1c00430

[10] Pan, Yong, Tengyang Zhu, Qing Xia, Xi Yu, and Yan Wang. "Constructing superhydrophobic ZIF-8 layer with bud-like surface morphology on PDMS composite membrane for highly efficient ethanol/water separation." *Journal of Environmental Chemical Engineering* 9, no. 1 (2021): 104977. https://doi.org/10.1016/j.jece.2020.104977

[11] Genix, Anne-Caroline, Vera Bocharova, Bobby Carroll, Philippe Dieudonné-George, Edouard Chauveau, Alexei P. Sokolov, and Julian Oberdisse. "Influence of the graft length on nanocomposite structure and interfacial dynamics." *Nanomaterials* 13, no. 4 (2023): 748. https://doi.org/10.3390/nano13040748

[12] Saito, Takamasa, Eita Shoji, Masaki Kubo, Takao Tsukada, Gota Kikugawa, and Donatas Surblys. "Evaluation of the work of adhesion at the interface between a surface-modified metal oxide and an organic solvent using molecular dynamics simulations." *The Journal of chemical physics* 154, no. 11 (2021). https://doi.org/10.1063/5.0040900

[13] Gao, Pan, Wei Pu, Pengchong Wei, and Miqiu Kong. "Molecular dynamics simulations on adhesion energy of PDMS-silica interface caused by molecular structures and temperature." *Applied surface science* 577 (2022): 151930. https://doi.org/10.1016/j.apsusc.2021.151930

[14] Pang, Honglei, Yayu Qiu, and Weipeng Sheng. "Long-term stability of PVDF-SiO2-HDTMS composite hollow fiber membrane for carbon dioxide absorption in gas–liquid contacting process." *Scientific Reports* 13, no. 1 (2023): 5531. https://doi.org/10.1038/s41598-023-31428-8

[15] Gao, Ming, Yuanlu Zhu, Jiangyi Yan, Weixing Wu, and Beifu Wang. "Micromechanism study of molecular compatibility of PVDF/PEI blend membrane." *Membranes* 12, no. 8 (2022): 809. https://doi.org/10.3390/membranes12080809

[16] Hu, Jianping, Zhen Fang, Yanfen Huang, and Jiazheng Lu. "Fabrication of superhydrophobic surfaces based on fluorosilane and TiO2/SiO2 nanocomposites." *Surface Engineering* 37, no. 3 (2021): 271-277. https://doi.org/10.1080/02670844.2020.1730059

[17] Su, Guirong, Sha Yang, Yingda Jiang, Jingtai Li, Shuang Li, Ji-Chang Ren, and Wei Liu. "Modeling chemical reactions on surfaces: The roles of chemical bonding and van der Waals interactions." *Progress in Surface Science* 94, no. 4 (2019): 100561. https://doi.org/10.1016/j.progsurf.2019.100561

[18] Tan, J. Y., W. L. Ang, and A. W. Mohammad. "Hydrophobic polyvinylidene fluoride membrane modified with silica nanoparticles and silane for succinic acid purification using osmotic distillation process." *J. Kejuruter* 33 (2021): 89-101. https://doi.org/10.17576/jkukm-2021-33(1)-10

[19] Yadav, Pooja, Ramin Farnood, and Vivek Kumar. "Superhydrophobic modification of electrospun nanofibrous Si@ PVDF membranes for desalination application in vacuum membrane distillation." *Chemosphere* 287 (2022): 132092. https://doi.org/10.1016/j.chemosphere.2021.132092

[20] Luo, Qi, Yiping Xie, Qixia Nie, Qingrui Yang, and Xinyu Zhang. "Impact of pore sizes and defects on CSH/epoxy bonding in wet conditions: A molecular dynamics analysis." *Next Materials* 5 (2024): 100253. https://doi.org/10.1016/j.nxmate.2024.100253

[21] He, Qiuping, Wei Chen, Pengfei Wang, and Xiaoming Dou. "Silicalite-1/PDMS hybrid membranes on porous PVDF supports: preparation, structure and pervaporation separation of dichlorobenzene isomers." *Polymers* 14, no. 9 (2022): 1680. https://doi.org/10.3390/polym14091680

[22] Hamouni, Samia, Omar Arous, Djamel Abdessemed, Ghania Nezzal, and Bart Van der Bruggen. "Alcohol and alkane organic extraction using pervaporation process." In *Macromolecular Symposia*, vol. 386, no. 1, p. 1800247. 2019. https://doi.org/10.1002/masy.201800247

[23] Mamah, Stanley Chinedu, Pei Sean Goh, Ahmad Fauzi Ismail, Be Cheer Ng, Mohd Sohaimi Abdullah, Nor Akalili Ahmad, Muhammad Hafizuddin Hazaraimi, and Athirah Mohd Tamidi. "Advancement in modification of polyvinylindene flouride hollow fiber membrane contactors for CO2 capture." *Emergent Materials* (2025): 1-25. https://doi.org/10.1007/s42247-025-01059-y

[24] Liu, Wei-Min, Heng Mao, Yu-Jie Wang, Shen-Hui Li, Ying-Nan Feng, Li-Hao Xu, Sen Wang, Chan Pei, and Zhi-Ping Zhao. "Fabrication of highly permeable PDMS@ ZIF-8/PVDF hollow fiber composite membrane in module for ethanol-water separation." *AIChE Journal* 69, no. 9 (2023): e18120. https://doi.org/10.1002/aic.18120